Pergamon

Chaos, Solitons & Fractals Vol. 5, No. 10, pp. 2003–2011, 1995

0960–0779/95$9.50 + .00

0960–0779(94)00179-0

Chaos–Hyperchaos Transition

T. KAPITANIAK,* K.-E. THYLWE,† I. COHEN† and J. WOJEWODA‡

†Department of Mechanics, Royal Institute of Technology, 100 44 Stockholm, Sweden, and *Division of Control and Dynamics, Technical University of Łódź, Stefanowskiego 1/15, 90-924 Łódź, Poland

Abstract—We discuss properties of an attractor in the neighbourhood of chaos–hyperchaos transition. The intermittency like model and a scaling law for the transition based on the features of the Poincaré map are developed. We investigate the properties of the Lyapunov and correlation dimensions in the neighbourhood of the transition point.

1. INTRODUCTION

In the last two decades it has been shown that chaotic behaviour is typical for three-dimensional dynamical systems. The chaotic attractor is characterized by one positive Lyapunov exponent indicating sensitive dependence on initial conditions (exponential spreading within the attractor in the direction transverse to the flow). In higher (at least four) dimensional systems beside chaotic attractors it is possible to find hyperchaotic attractors with two positive Lyapunov exponents [1–5]. Such attractors involve two directions of spreading within the attractor.

In this paper we investigate properties of the transition from chaos to hyperchaos for two coupled systems,

$$\begin{aligned} \ddot{x} - a(1 - x^2)\dot{x} + x^3 &= b(\sin \omega t + y) \\ \ddot{y} - a(1 - y^2)\dot{y} + y^3 &= b(\sin \omega t + x) \end{aligned} \tag{1}$$

where a, b and ω are constant and

$$\begin{aligned} \ddot{x} + \alpha\dot{x} + x^3 &= B \cos \omega t \\ \ddot{y} + \beta\dot{y} + y^3 &= x \end{aligned} \tag{2}$$

where α, β, B and ω are constant. In numerical investigations we considered $a = 0.2$, $\omega = 4.0$ and b as control parameter in equations (1) and $\alpha = 0.1$, $B = 10.0$, $\omega = 1.0$ and β as a control parameter in equations (2).

The first system represents two coupled generalized van der Pol equations and was originally investigated in [4]. The second one can be interpreted as Duffing's equation (the second equation in (2)) forced by chaotic ouput from another Duffing's equation (the first equation in (2)). It should be noted here that chaotic forcing has some practical advantages in comparison with periodic one. Using chaos we can, for example, correct certain nonlinear out-of-phase problems, eliminate fractal basin boundaries [6] and control unstable orbits [7]. The dynamics of chaotically forced systems is strictly connected with chaotic signals synchronization phenomenon [8–10].

The structure of the phase-space of both systems indicates that one of the Lyapunov exponents must be zero. As well as the typical chaotic attractors (with one positive

Lyapunov exponent (+, 0, −, −, −)) it is possible to find hyperchaotic attractors with two positive Lyapunov exponents. Positive Lyapunov exponents indicate exponential spreading within the attractor in directions transverse to the flow and negative exponents indicate exponential contraction onto the attractor. Under the action of such a flow, phase-space volumes evolve in the way schematically shown in Fig. 1 (spreading in directions x and y, contraction in directions x and y).

The plan of the paper is as follows. In Section 2 we investigate the properties of the projections of Poincaré map of chaotic and hyperchaotic attractors in the neighbourhood of the transition point. The scaling law for transition from chaos to hyperchaos for both systems (1) and (2) is described. Section 3 presents the properties of Lyapunov and correlation dimensions at the transition point. We show that Lyapunov dimension is a continuous function of the control parameter and that the correlation dimension exhibits one scaling region for chaotic attractor and two scaling regions for hyperchaos. Finally we summarize our results in Section 4.

2. PRECHAOS–HYPERCHAOS INTERMITTENCY

Projections of Poincaré maps onto the plane $x-y$ for equations (1) are shown in Fig. 2 and for equations (2) in Fig. 3. In Figs 2(a) and 3(a) we showed projections of Poincaré maps of the chaotic attractor, while in Figs 2(b) and 3(b) Poincaré maps describe hyperchaotic behaviour.

If we compare Figs 2(a) and 3(a) with Figs 2(b) and 3(b) we find that in a chaotic case we can observe domains of Poincaré map (denoted by A in Fig. 2(c)) where the concentration of points is greater than in other parts of the map (denoted by B in Fig. 2(c)). In the hyperchaotic example we have no such domains. The successive Poincaré map point of the chaotic trajectory stays in the domain A for a relatively long time and escapes

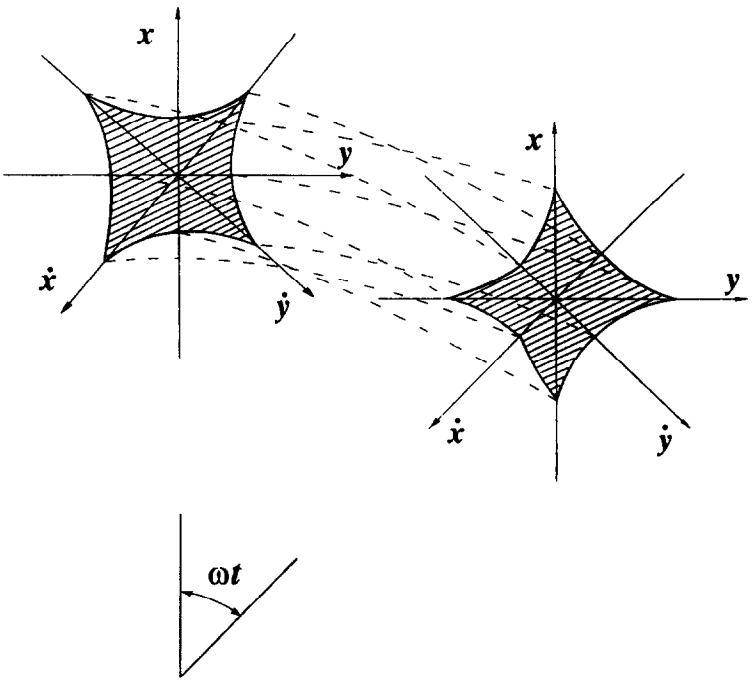

Fig. 1. Schematic evolution of phase-space under the action of hyperchaotic flow.

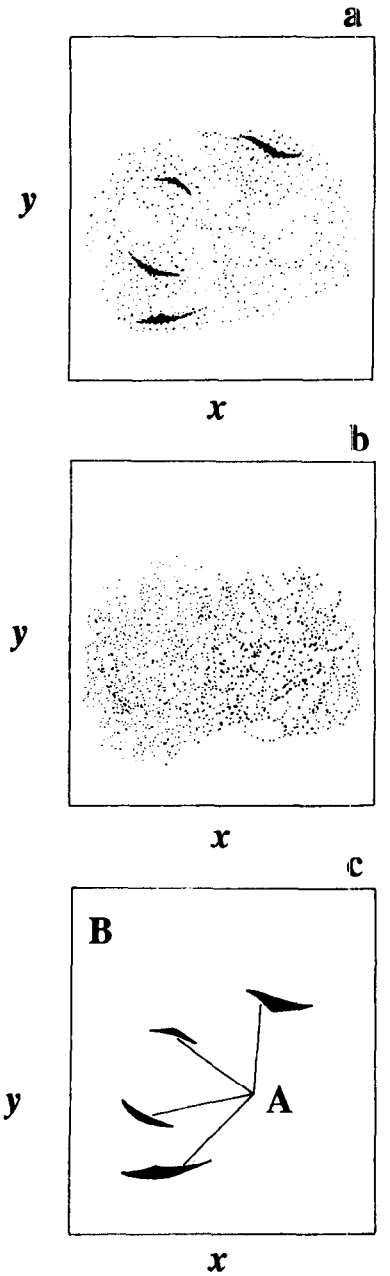

Fig. 2. Projections of the Poincaré map of the system (1) $a = 0.2$, $\omega = 4.0$: (a) chaotic behaviour $b = 6.0$, (b) hyperchaotic behaviour $b = 7.0$, (c) domains A and B.

from it to domain B for a much shorter time after which it comes back to A. Numerically, domain A has been estimated in the following way. After cutting the transient we observed the Poincaré map for a number of periods T (in the presented examples $T = 10^6$). This observation allowed us to define domain A and further observation gives us the following symbolic dynamics:

1: the point of the Poincaré map is in domain A,
0: the point of the Poincaré map is in domain B.

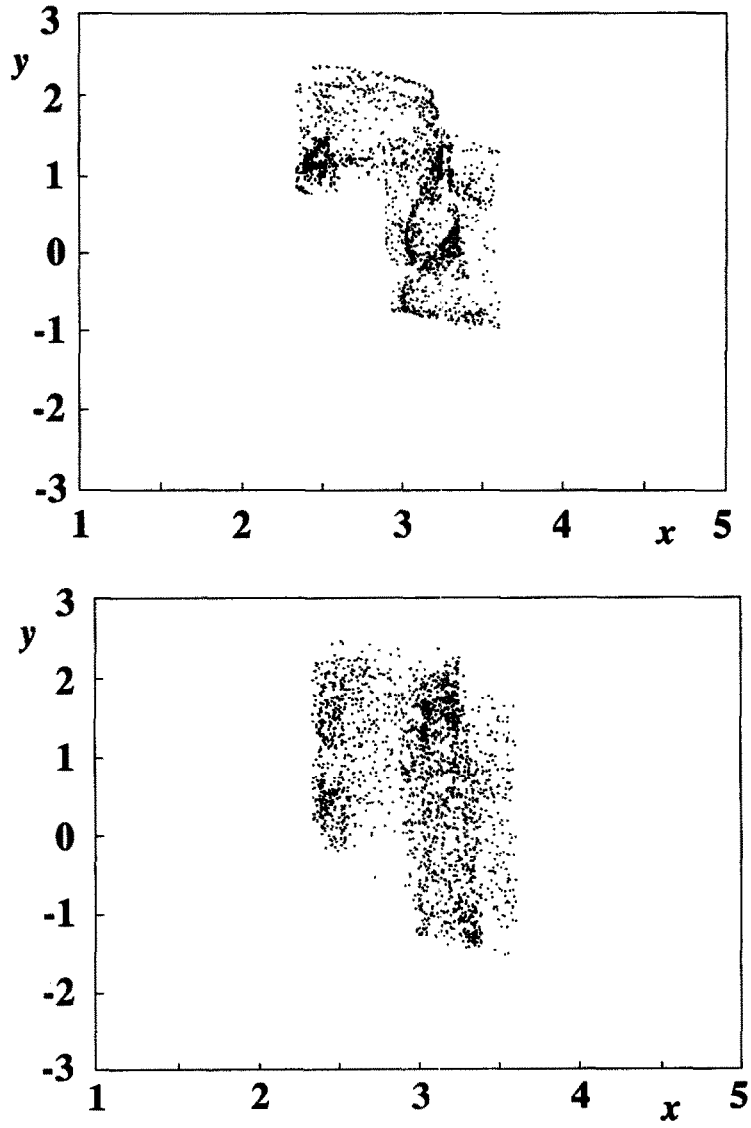

Fig. 3. (a) Projection of the Poincaré map of the system (2)—chaotic behaviour $\beta = 0.2$. (b) Projection of the Poincaré map of the system (2)—hyperchaotic behaviour $\beta = 0.1$.

For example for the system (1) with $b = 5.2$ we have the following sequence of symbols,

$(1111 \ldots 1)$	$(0 \ldots 0)$	$(1111 \ldots 1)$	$(0 \ldots 0)$	$\ldots$
$(10^4 + 120)T$	$34T$	$(10^4 + 78)T$	$43T$	

The numbers given under each sequence in parentheses indicate the number of periods T for which each sequence takes place.

Let R be an average number of periods T for which the trajectory stays outside domain A. If we are increasing the value of control parameters (b in equations (1) and β in (2)) towards the values which are the boundaries of hyperchaos we observe that R increases and we found the following scaling laws for transition from chaos to hyperchaos,

$$R \sim (b - b_c)^{-\zeta}$$

and

$$R \sim (\beta - \beta_c)^{-\zeta}$$

where b_c and β_c are critical values of control parameters at which the transition to hyperchaos occurs. We found $\zeta = 0.72 \pm 0.02$ for both equations (1) and (2). Similar relations can be obtained by the investigation of other projections of the Poincaré map. It is interesting that for two different systems (1) and (2) we found similar values of ζ, although it is too early to speculate possible universality.

Presented properties of the projections of Poincaré map suggest the mechanism of chaos–hyperchaos transition similar to the mechanism of the classical intermittency [11] with the long evolution in domain A with occasional bursts to the domain B. We proposed to call this mechanism prechaos–hyperchaos intermittency, as this phenomenon takes place before transition.

The simple way of coupling in equations (1 and 2) does not allow direct observation of the increase of the dimensionality of the attractor after transition to hyperchaos on the projections of the Poincaré map. Recently such an observation was found to be possible in a chaos synchronization schemes [21]. We comment on this problem in Section 4.

3. DIMENSIONS OF ATTRACTORS AT TRANSITION

Equations (1) and (2) have the Lyapunov exponents spectrum consisting of five exponents and Lyapunov dimensions associated with them

$$d_L = j + \frac{\sum_{i=1}^{j} \lambda_i}{|\lambda_{j+1}|} \tag{3}$$

where j is determined by $\sum_{i=1}^{j} \lambda \geq 0$ but $\sum_{j=1}^{N+1} \lambda < 0$. According to the Kaplan–Yorke conjecture [12] $d_L = d_I$, where d_I is an information dimension. Information and Lyapunov dimensions are related to the other attractor's dimensions as follows:

$$d_C \geq d_I \approx d_L \geq d_{corr}$$

where d_C is a capacity dimension, while d_{corr} is a correlation dimension [13]. Until now there has been no effective way of estimating the capacity dimension of attractors of higher dimensional systems, and this dimension will not be considered here. The correlation dimension, the second attractor dimension measure which we consider in this paper, is defined in terms of the scaling behaviour of the so-called correlation integral. For a $d = 2N + 1$ dimensional embedding with trajectory vectors x_k we define the correlation sum as

$$C_d(R) = \sum_{k,l=1,k\neq l}^{M} \Theta(R - |x_k - x_l|) \tag{4}$$

where M is the number of vectors in the data set being analysed and Θ is the Heaviside step function. As it is well known, the correlation integral $C_d(R)$ gives the average of the relative number of trajectory points within the distance R of another trajectory point. For many attractors, the correlation dimension is defined as that number which satisfies

$$d_{corr} = \frac{\log C(R)}{\log R} \tag{5}$$

in the scaling region. In practical situations the scaling region can be rather limited [14, 15].

For large R, larger than the size of the attractor, the correlation integral saturates at the value of unity. For small R, smaller than the smallest distance between data points, the integral goes to zero. Despite these inconveniences the correlation dimension has been found as the simplest characterization of experimental attractors, for example in refs [16, 17] while estimation of Lyapunov exponents from time series can sometimes lead to incorrect results [17, 18].

For example let us consider equations (2). The trajectories of the first equation of (2) are located on the 3D manifold. If the trajectories of the whole system (2) are located in this 3D manifold as well, then the second equation simply reproduces the chaotic oscillations of the first oscillator as all trajectories converge to the attractor of the first equation (2). The described manifold exists for any value of the coupled oscillators parameter β. This enables us to investigate the stability of the chaotic limit set located in this manifold as a function of β. The Lyapunov exponents spectrum of the coupled system (2) can be divided into two subsets $\lambda^{(1)}$ and $\lambda^{(2)}$, respectively along and orthogonal to the manifold. The first subset of Lyapunov exponents is associated with driving system (the first equation of (2)) and consists of three exponents describing the evolution of perturbations tangent to the manifold. The Lyapunov exponents of the second subset (the second equation of (2)) describe the evolution of the perturbations transverse to the manifold. As was shown recently by de Sousa [10], they are equivalent to the conditional or sub-Lyapunov exponents of Pecora and Carroll [8]. The dependence of the Lyapunov dimension on β (curbe b) or b (curve a) is presented in Fig. 4 where we have also indicated the intervals where the Lyapunov exponents spectrum has one (solid line), two (broken line) positive exponents.

Lyapunov exponents have been computed using a software INSITE [20]. Computations have been performed with a β(b)-step equal to 0.005 in the whole interval and with a step 0.0005 in the neighbourhood of chaos–hyperchaos transition. It clearly appears that in the case of equation (2) there is a region for higher values of β where all $\lambda^{(2)}$-Lyapunov exponents are negative (β interval: [0.121, 0.2]). In this interval the chaotic limit set of the whole system (2) is located on the manifold of the attractor of the forcing system (the first

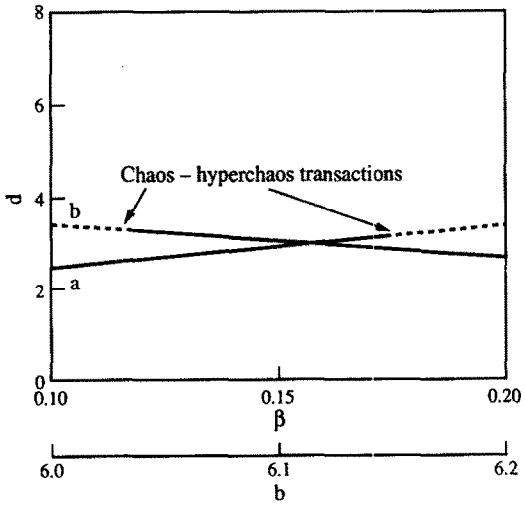

Fig. 4. Lyapunov dimension versus β and b plots; curve a: equation (1): $\alpha = 0.2$, $\omega = 4.0$, curve b: equation (2): $\alpha = 0.1$, $B = 10.0$, $\omega = 1.0$.

equation in (2)). For the smaller values of β at least one $\lambda^{(2)}$-Lyapunov exponent is positive and the resulting limit set is not restricted to the manifold of the forcing subsystem, and we observe a hyperchaos regime. From Fig. 4 one can find that the Lyapunov dimension-control parameter β or b relation is a continuous function at the transition point from chaos to hyperchaos. Figure 5 (a, b) presents log–log plots of the correlation integral (3) as a function of the distance R. In Fig. 5(a) the plot shows the results for the chaotic case (only one positive Lyapunov exponent) while in Fig. 5(b) we present a hyperchaotic case with two positive Lyapunov exponents.

From these plots one can find that in the case of chaos, the correlation integral exhibits only one scaling region, while for hyperchaotic case two scaling regions are visible. As shown before, in the chaotic case the trajectories of all oscillators evolve on the 3D manifold of the first attractor, and their behaviour is strongly connected (all oscillators evolve in the same region of the phase-space—on the attractor of forcing oscillator). In the hyperchaotic case other oscillators evolve in the larger dimensional manifolds and their behaviour is less connected with the behaviour of the first one (forced oscillators do not evolve on the same attractor as a forcing oscillator). With this interpretation our results can be explained in terms of Lorenz conjectures [15].

The robustness of our conjecture that d_L (control parameter) is a continuous function

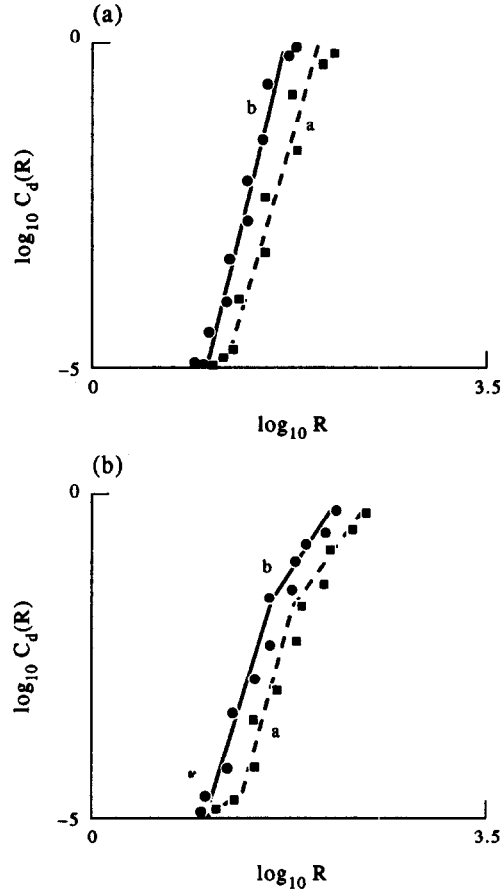

Fig. 5. Log-log plot of correlation integral vs. distance R for equations (2): (a) chaotic regime $b = 6.10$—equations (1), $\beta = 0.122$—equations (2); (b) hyperchaotic regime $b = 6.20$—equations (1), $\beta = 0.120$—equations (2).

and that the correlation dimension shifts from one to two scaling regions at the transition from chaotic to hyperchaotic behaviour, was confirmed in system (1) where two oscillators are mutually coupled (curve (a) in Fig. 5 and 6(a, b)) and in [15] where we considered the system of a chain of unidirectionally coupled oscillators at the chaos–hyperchaos boundary.

4. CONCLUSIONS

It has been demonstrated here that the chaos–hyperchaos transition can be described by the properties of a Poincaré map. We proposed the intermittency mechanism and found a scaling law describing this transition. However, for simply coupled systems such as equations (1) and (2) it is impossible to observe directly the increase of dimensionality of the attractor as is possible in the case of feedback coupling mechanism of two chaotic systems $\dot{x} = f(x)$ and $\dot{y} = f(y)$, i.e.

$$\dot{x} = f(x) + K(y - x) \tag{6a}$$

$$\dot{y} = f(y) \tag{6b}$$

where $x, y \in \mathbb{R}^3$, K is a constant. In such systems it is possible to find a value of K for which both systems (6a) and (6b) synchronize. In this case the coupled system (6) is characterized by one positive Lyapunov exponent (in the $\lambda^{(1)}$ subset) and $x-y$ projection of the attractor is simply a line (one-dimensional structure). If we have hyperchaotic regime, one of the Lyapunov exponents in the $\lambda^{(2)}$ subset must be positive, so we have no synchronization and $x-y$ projection represents a two-dimensional structure [21].

Chaotic and hyperchaotic regimes can be distinguished by the knowledge of the whole spectrum of Lyapunov exponents. Unfortunately, this distinction cannot be made based on the Lyapunov dimension d_L or associated with its information dimension d_I, as the dependence of d_L on the system control parameter has been found as a continuous function at the chaos–hyperchaos boundary for both periodic and chaotic forcing. This result is not trivial and quite surprising, as the information dimension of the attractor plays a crucial role in the experimental distinction between strange chaotic and strange nonchaotic attractors [17, 20]. The correlation dimension allows follow up of the distinction between chaotic and hyperchaotic regimes, as we observe a different number of scaling regions in both regimes. This property can be useful to follow up the chaos–hyperchaos distinction based on a single experimental time series.

REFERENCES

1. O. E. Rossler, *Z. Naturforsch. a* **38**, 788–801 (1983).
2. O. E. Rossler, *Phys. Lett. A* **71**, 155 (1979).
3. K. Kaneko, *Prog. Theor. Phys.* **69**, 1427 (1983).
4. T. Kapitaniak and W.-H. Steeb, *Phys. Lett. A* **152**, 33 (1991).
5. T. Kapitaniak, *Phys. Rev. E* **47**, R2975 (1993).
6. L. Pecora and T. S. Carroll, *Phys. Rev. Lett.* **67**, 945–948 (1991).
7. E. Ott, C. Grebogi and Y. A. Yorke, *Phys. Rev. Lett.* **64**, 1196 (1990).
8. L. Pecora and T. S. Carroll, *Phys. Rev. Lett.* **64**, 821–824 (1990).
9. L. Pecora and T. S. Carroll, *IEEE Trans. Circuits and Systems* **38**, 453–456, (1991).
10. M. de Sousa, A. J. Lichtenberg and M. A. Lieberman, Self-synchronization of many coupled oscillators, Memorandum No. UCB/ERL M92/20, (1992).
11. T. Kapitaniak, *Chaotic Oscillations in Mechanical Systems*. Manchester University Press, Manchester (1991).
12. J. L. Kaplan and J. A. Yorke, in *Functional Differential Equations and Approximations of Fixed Points*, edited by H. O. Peitgen, and H. O. Walther, Springer, Berlin (1979).
13. P. Grassberger and I. Procacia, *Phys. Rev. Lett.* **50**, 346–349 (1983).

14. N. B. Abraham, A. M. Albano, B. Das, G. DeGuzman, S. Yong, R. S. Gioggia, G. R. Puccioni and J. R. Tredice, *Phys. Lett. A* **114**, 217–221 (1986).
15. E. Lorenz, *Nature, Lond* **353**, 241–244 (1991).
16. J. Wojewoda, T. Kapitaniak, R. Barron and J. Brindley, *Chaos, Solitons & Fractals* **3**, 35 (1993).
17. T. Kapitaniak, *Chaos, Solitons & Fractals* **1**, 67–77.
18. T. Kapitaniak and M. S. El Naschie, *Phys. Lett. A* **154** 249–254 (1991).
19. T. S. Parker and L. O. Chua, *Practical Numerical Algorithms for Chaotic Systems*, Springer, New York (1989).
20. W. L. Ditto, M. L. Spano, H. T. Savage, S. W. Rauseo, J. Heagy and E. Ott, *Phys. Rev. Lett.* **65**, 533–535 (1990).
21. T. Kapitaniak and L. O. Chua, *Int. J. Bifurcation and Chaos* **4**, 477–483 (1994).